

An Examination of Soil Crusts on the Floor of Jezero crater, Mars

E.M. Hausrath¹, C.T. Adcock¹, A. Bechtold², P. Beck³, K. Benison⁴, A. Brown⁵, E.L. Cardarelli⁶, N.A. Carman¹, B. Chide⁷, J. Christian⁸, B.C. Clark⁹, E. Cloutis¹⁰, A. Cousin¹¹, O. Forni¹¹, T.S.J. Gabriel¹², O. Gasnault¹¹, M. Golombek⁶, F. Gómez¹³, T.L.J. Henley¹⁴, J. Huidobro¹⁵, J. Johnson¹⁶, M. W. M. Jones¹⁷, T.V. Kizovski¹⁴, A. Knight⁸, J.A. Lasue¹¹, S. Le Mouélic¹⁸, J.M. Madariaga¹⁵, J. Maki⁶, L. Mandon¹⁹, G. Martinez²⁰, J. Martínez-Frías²¹, T. McConnochie⁹, P-Y. Meslin¹¹, M-P. Zorzano Mier¹³, G. Paar²³, C. Royer²⁴, S. Siljeström²⁵, M.E. Schmidt¹⁴, S. Schröder²², M.A. Sephton²⁶, R. Sullivan²⁷, N. Turenne¹⁰, A. Udry¹, S. VanBommel⁸, A. Vaughan¹², R.C. Wiens²⁸, N. Williams⁶, the SuperCam team and the Regolith working group

¹Department of Geoscience, University of Nevada, Las Vegas, Nevada 89154, USA.

²Department of Lithospheric Research, University of Vienna, Austria.

³Institut de Planétologie et d'Astrophysique, de Grenoble, University of Grenoble Alpes, France.

⁴Department of Geology and Geography, West Virginia, University, Morgantown, West Virginia 26506, USA.

⁵Plancius Research, Severna Park, Maryland, USA.

⁶NASA Jet Propulsion Laboratory, California Institute of Technology, Pasadena, CA 91109

⁷Los Alamos National Laboratory, Los Alamos, New Mexico, 87545, USA.

⁸Department of Earth and Planetary Sciences, Washington University in St. Louis, Missouri 63130, USA.

⁹Space Science Institute, Boulder, Colorado 80301, USA.

¹⁰ Department of Geography, University of Winnipeg, Winnipeg, Manitoba, R3B 2E9, Canada.

¹¹Institut de Recherche en Astrophysique et Planétologie, 31400 Toulouse, France.

¹²US Geological Survey, LLC, Flagstaff 86001, Arizona, USA.

¹³Centro de Astrobiología (CSIC-INTA), Torrejón de Ardoz, Madrid, Spain.

¹⁴Department of Earth Science, Brock University, St. Catharines, Ontario L2S 3A1, Canada.

¹⁵Department of Analytical Chemistry, University of the Basque Country UPV/EHU, 48940 Leioa, Spain.

¹⁶John Hopkins University Applied Physics Laboratory, Laurel 20723, Maryland.

¹⁷Central Analytical Research Facility and School of Chemistry and Physics, Queensland University of Technology, Brisbane, QLD 4001, Australia.

¹⁸ Nantes Université, Univ Angers, CNRS, UMR 6112, Laboratoire de Planétologie et Géosciences, F-44000 Nantes, France

¹⁹ Université de Lyon, UCBL, ENSL, CNRS, LGL-TPE, 69622 Villeurbanne, France. N

²⁰ Lunar and Planetary Institute, Houston, Texas 77058, USA.

²¹ Instituto de Geociencias, Madrid, Spain.

²² DLR-OS, Berlin

²³ Joanneum Research, Graz, Austria.

²⁴ LESIA, Observatoire de Paris, Université PSL, CNRS, Sorbonne Université, Université de Paris, Meudon, France.

²⁵ RISE Research Institutes of Sweden, Stockholm, Sweden.

²⁶ Department of Earth Science & Engineering, Imperial College, London, UK.

²⁷ CCAPS, Cornell University, Ithaca, New York 14853, USA.

²⁸ Earth, Atmospheric and Planetary Sciences, Purdue University, West Lafayette, Indiana, USA

Corresponding author: Elisabeth Hausrath (Elisabeth.Hausrath@unlv.edu)

Contents of this file

Text S1

Figures S1 to S7

Tables S1 to S5

Additional Supporting Information (Files uploaded separately)

Table S1. The retrieved H component

Table S2. Additional data and figures for soil crust and wheel tracks

Table S3. The PIXL oxides data

Table S4. Members of the Regolith Working Group

Table S5. Members of the SuperCam team

Introduction

The information included here are figures used to support the text, figures, and tables in the main paper.

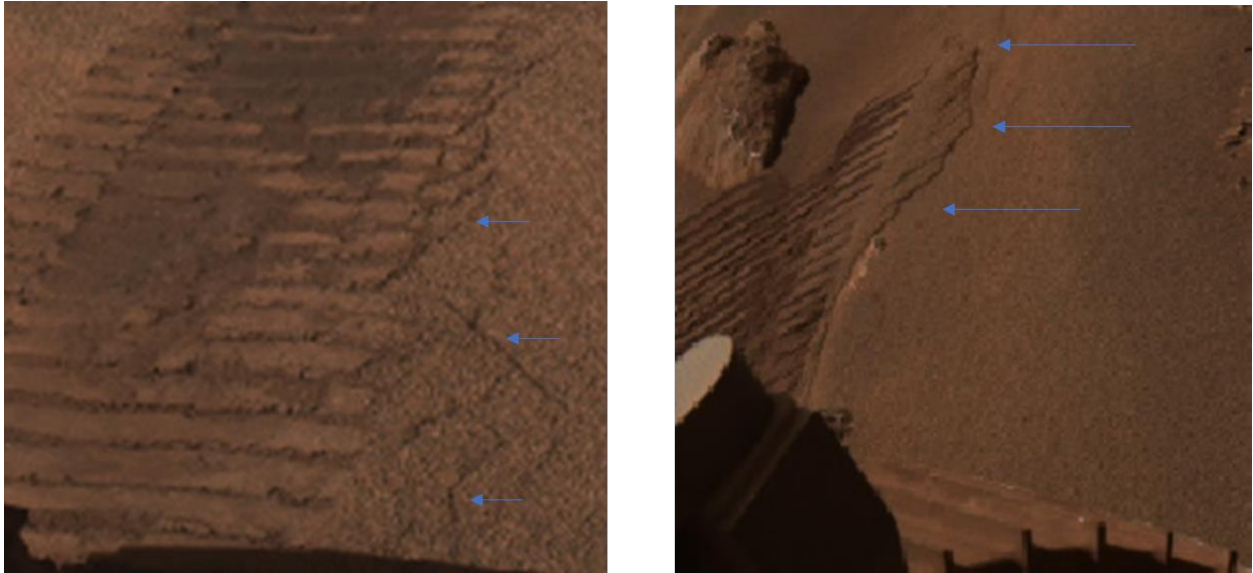


Figure S1. *Left:* Rear HazCam image of cracks (indicated with arrows) formed when the rover drove over the soil surface (for scale the rover wheel is 33.6 cm wide) from Sol 135 *Right:* Rear HazCam image of surface “rafting” formed when the rover drove over a crust from Sol 131.

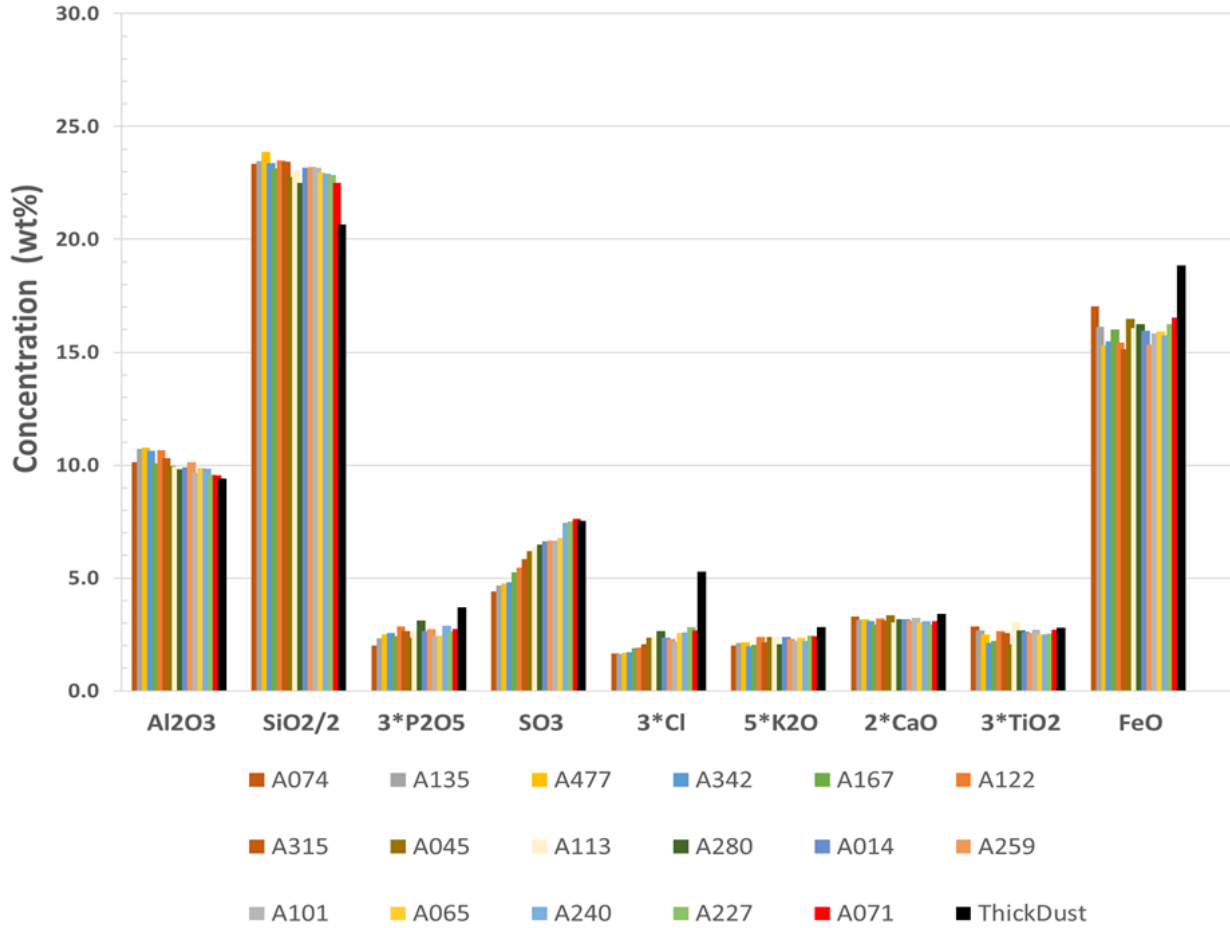


Figure S2. Global soils sorted by SO₃ increasing content, as measured by the Spirit rover mission. The Mars2020 target Naltsos “thick dust” values are the black bars on the far right of each element. Exaggeration of some elements is to facilitate compositional comparisons. The labels represent A for the Spirit rover, followed by the sol, and the data can be found in the PDS for that mission: https://pds-geosciences.wustl.edu/missions/mer/mer_apxs_oxide.htm.

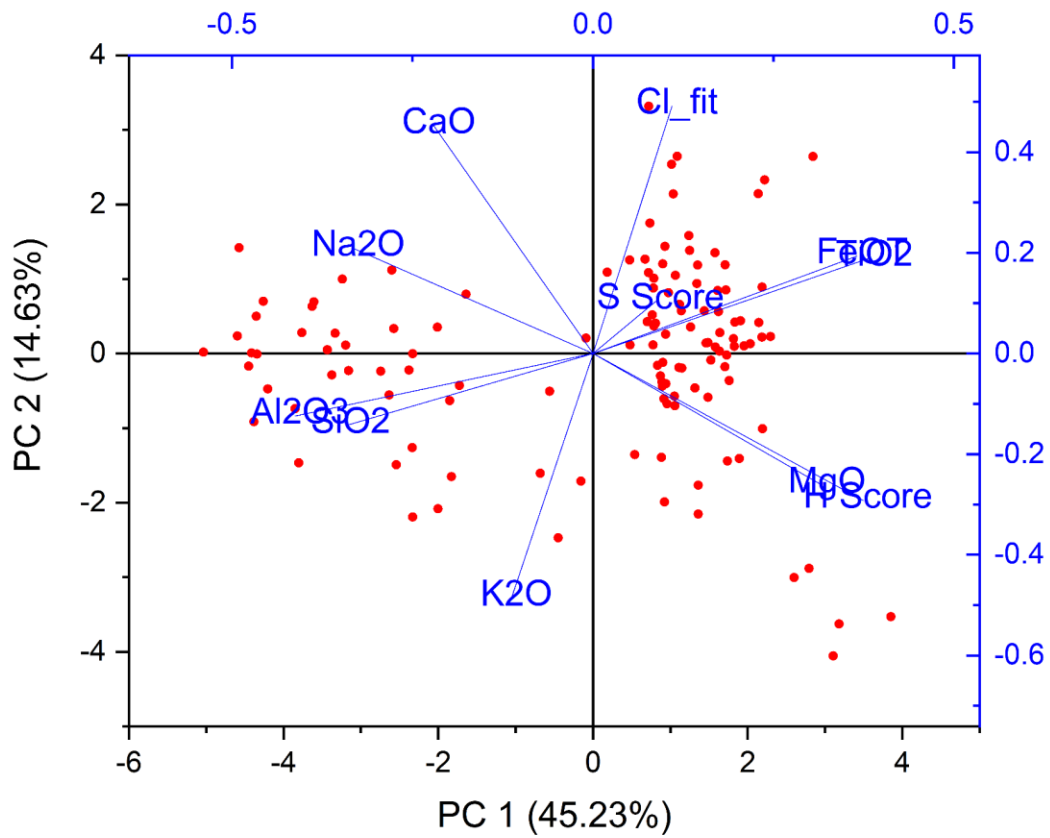


Figure S3. Tight correlation of Mg with S for the SuperCam points measured on the Mars2020 Target Naltsos suggest that the Mg sulfates observed by PIXL might be hydrated.

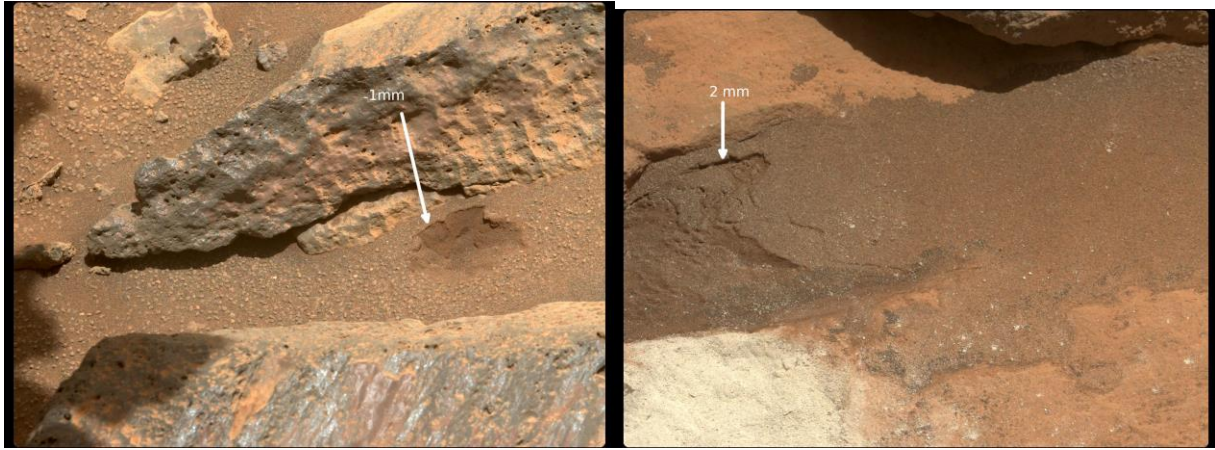


Figure S4. Quantification of the thickness of crusts disturbed during abrasion/coring on sols A) 188 and B) 207. Thicknesses of the crust quantified after Parr et al. (this issue), and C) Thickness of the crust that appears to have been disturbed not by the rover. The image IDs are: A) ZCAM08208 B) ZCAM08235 and C) ZCAM08367

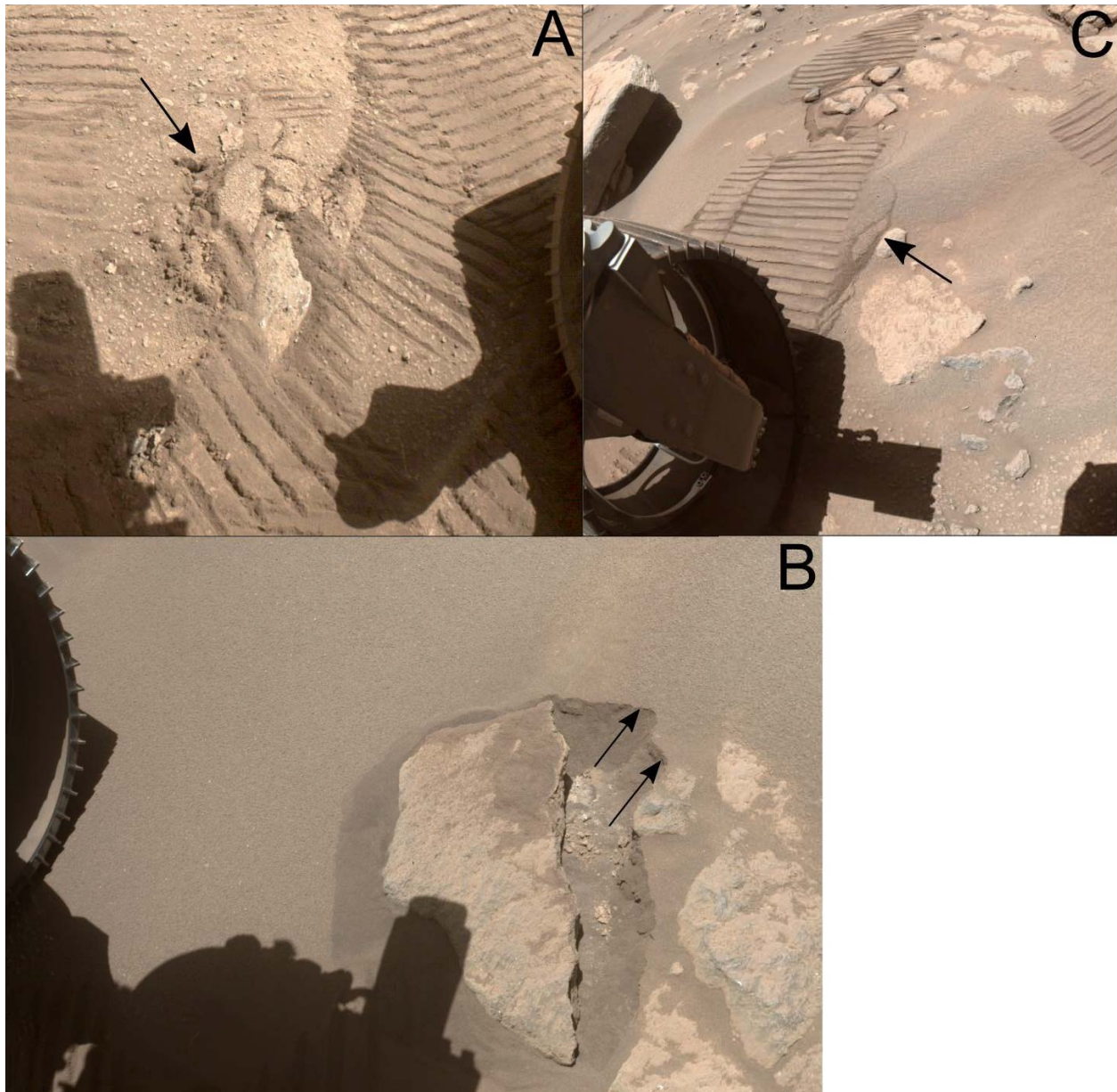
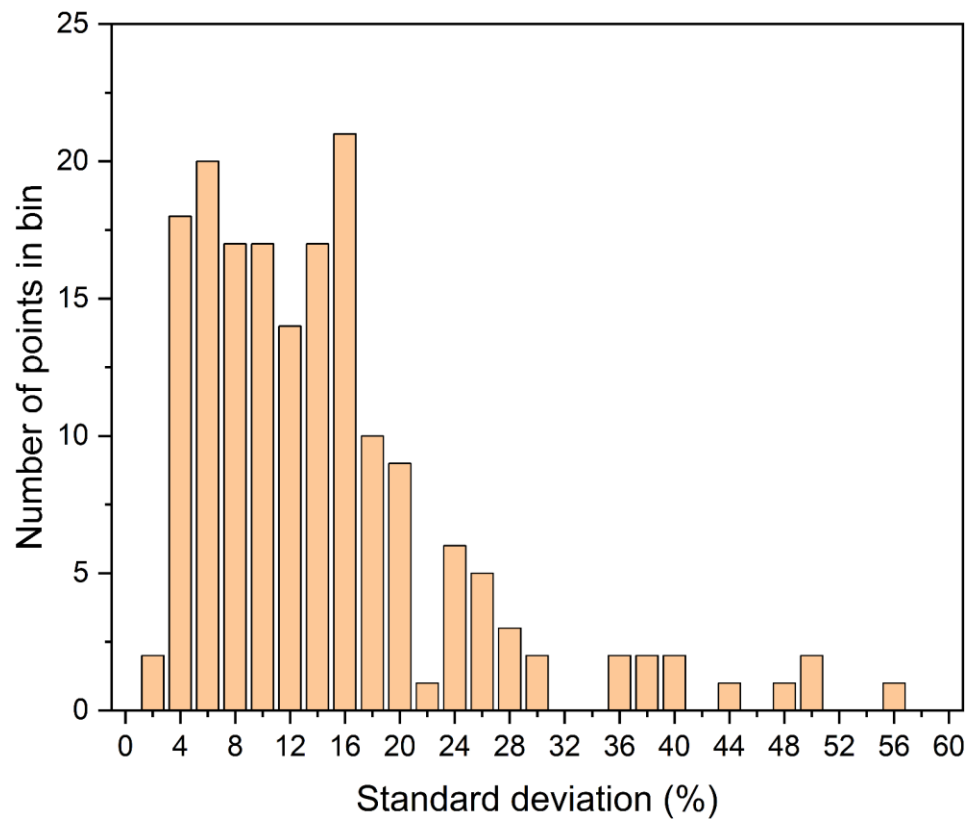


Figure S5. The crusts observed in flatter areas are typically fine-grained (A) or a mixture of fine and coarse grains (B) while the crusts observed on dunes are generally coarse-grained (C). Black arrows indicate crusts and associated grain sizes.

FLF_0031_0669694440_115CWS_N0030834FHAZ02005_0A1195J01

FLF_0275_0691348528_005CWG_N0080000FHAZ00300_0A00LLJ04

RLF_0278_0691618750_367CWG_N0080064RHAZ02419_0A0295J01



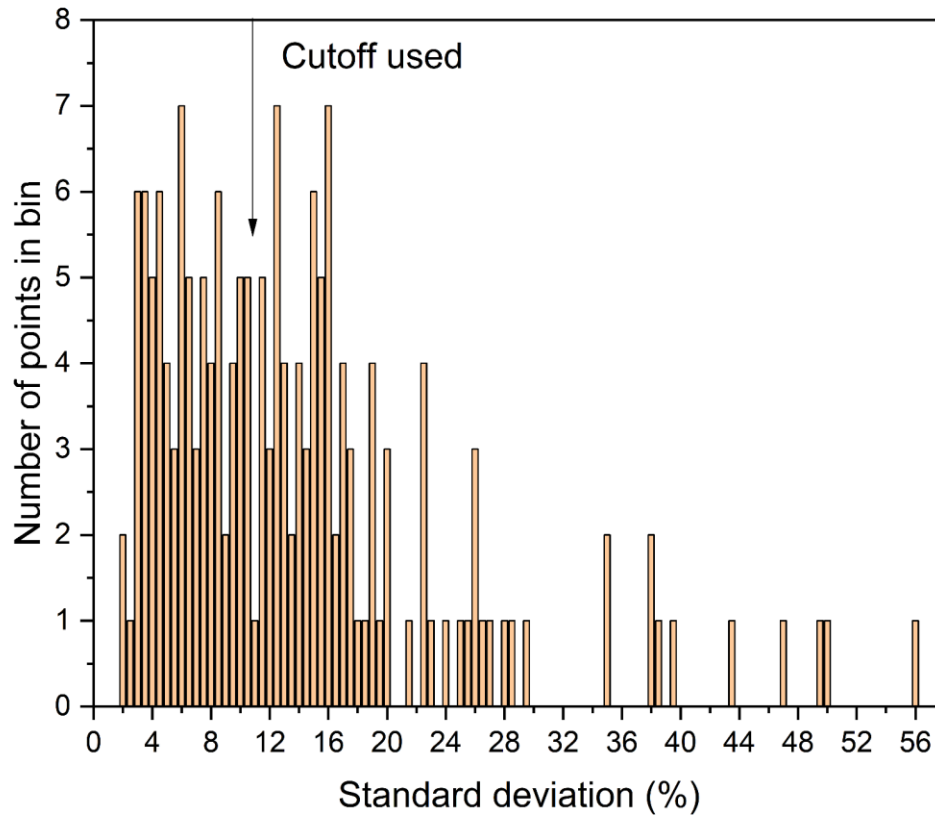


Figure S6. Figures showing the break between two potential groups, interpreted from the LIBS optical spectrum total emissivity, to help understand fine-grained versus coarse-grained material.

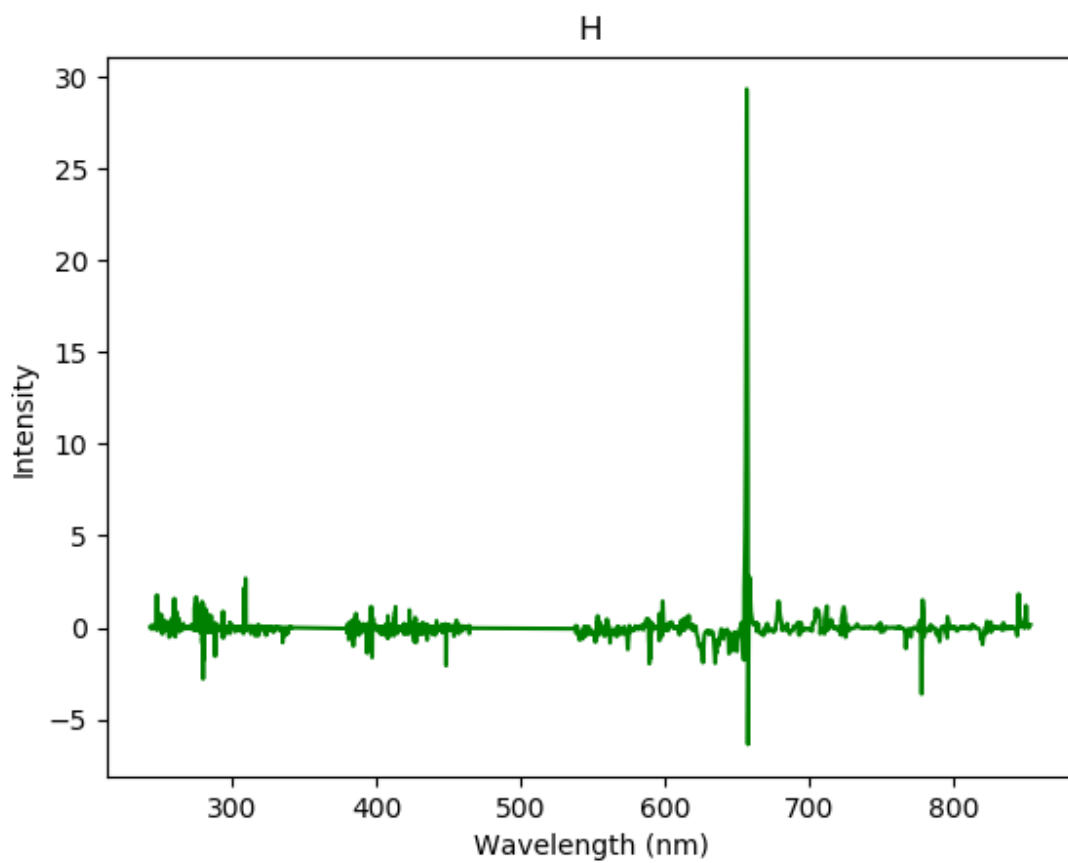


Figure S7. The retrieved H component used to tabulate the H scores after Forni et al. (2013).